The zfs parameter D (0.870 GHz) of SubPc is larger than that of ZntBPc, indicating that the extent of π delocalization in SubPc is much smaller than that of ZntBPc in the T_1 state. For SubPc, the ISC from the S_1 to the z sublevel of the T_1 state is selective. This selectivity is similar to ZntBPc but is contrary to MgtBPc or H_2tBPc. Calculations of the configurational interactions using the AM1 Hamiltonian have revealed that the E_x and E_y states are degenerate in both the S_1 (85%, HOMO-to-LUMO transition) and T_1 (97%, HOMO-to-LUMO transition) regions because of the degeneracy of the LUMOs (e_x and e_y), and that in the e MOs the population of the P_x and P_y orbitals are larger than that of the P_z orbital for both B and Br atoms. This can result in a z component of SOC between the $^{1,3}E_x$ and $^{3,1}E_y$ states originating from that between the e_x and e_y MOs. Using the SOC constants of the B ($=11$ cm^{-1}) and Br atoms ($=2460$ cm^{-1}), the SOC of the B and Br atoms is estimated as 0.013 and 0.28 cm^{-1}, respectively, indicating that the SOC on the Br atom is much larger than that of the B atom. Therefore, selective ISC of SubPc can be reasonably interpreted by SOC on the axial Br atom.

V. Phthalocyanine Dimers and Oligomers

The photophysical properties of Pc dimers and oligomers are important in relation to the photosynthesis and photonic wires, and have accordingly been intensively studied. In this section, the excited-state dynamics of Pc dimers and oligomers are introduced. First, the basic theory of homo dimers is explained in terms of exciton and charge resonance interactions. In Section V-B, photophysical properties of Pc dimers are discussed, focusing on the luminescence and transient absorption measurements. Recently, the TREPR method has been shown to be useful for clarifying the electronic structure of Pc dimers. Several TREPR studies on Pc dimers are discussed in Section V-C. In Section V-D, the excited-state dynamics of Pc oligomers are shown in relation to exciton transport and exciton–exciton annihilation. In the final section, Pc–Por hetero dimers and oligomers are discussed in terms of the electron and energy transfer processes. In particular, several light harvesting arrays and molecular photonic wires using Pcs as an energy acceptor have been reported, and the energy transfer process in these is discussed.

A. BASIC THEORY OF EXCITON AND CHARGE RESONANCE INTERACTIONS

The photophysical properties of dimers consisting of identical units can be analyzed by interplanar interactions between two Pc units, A and B, i.e. exciton (EX) and charge resonance (CR) interactions. All wavefunctions in the excited states are written as linear combinations of the EX and CR configurations, which are expressed as shown in eqs 6a and 6b:

$$^{1,3}\psi_{EX(\pm)} = (\psi_A^* \psi_B \pm \psi_A \psi_B^*)/\sqrt{2} \quad (6a)$$

$$^{1,3}\psi_{CR(\pm)} = (\psi_A^+ \psi_B^- \pm \psi_A^- \psi_B^+)\sqrt{2} \quad (6b)$$

Here, the superscripts *, +, and − denote the S_1 or T_1 state, and the ground states of the cation and anion of a Pc monomer, respectively. These configurations are shown in Scheme 1. The wavefunction of Pc dimers in the excited states, $^{1,3}\Psi_{DM}$, can be written as follows:

$$^{1,3}\Psi_{DM} = a^{1,3}\psi_{EX(\pm)} + b^{1,3}\psi_{CR(\pm)} \quad (7)$$

Since the Q band of Pcs is more intense than that of Pors,[3] the EX interaction in the S_1 state is important in Pc dimers. The EX interaction is approximated by the transition electric dipole–dipole interaction. Relationships between the dimer structure and EX interaction are shown in Figure 13. For the cofacial dimers (Figure 13A), the transition between the S_0 and upper EX states is electric-dipole allowed, while that between the S_0 and lower EX states is forbidden. In contrast, for the coplanar dimers (Figure 13B), the

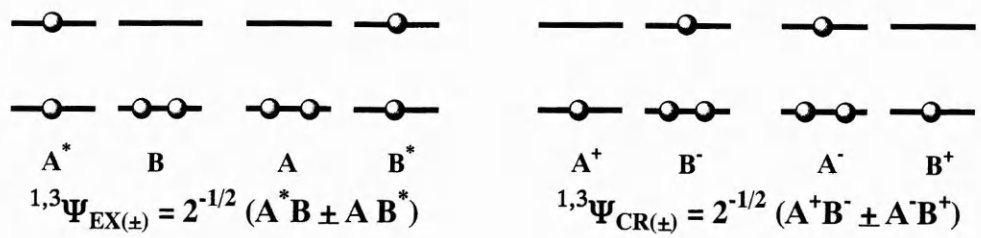

$$^{1,3}\Psi_{DM} = a\,^{1,3}\Psi_{EX(\pm)} + b\,^{1,3}\Psi_{CR(\pm)}$$

Scheme 1. Interactions of phthalocyanine dimer in the excited states.

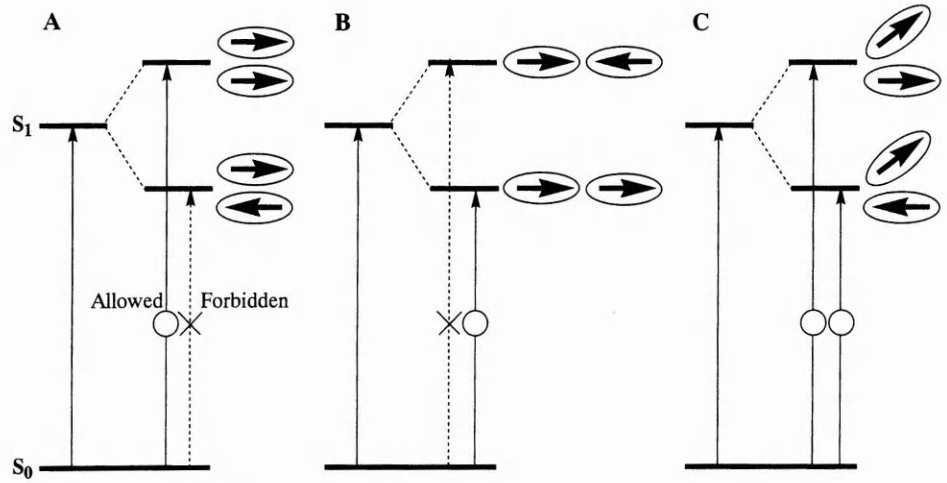

Figure 13. Relationships between the EX interaction and geometries. Cofacial (A), coplanar (B), and oblique dimers (C) are shown. Full and dashed arrows indicate electric-dipole allowed and forbidden transitions between the S_0 and EX states.

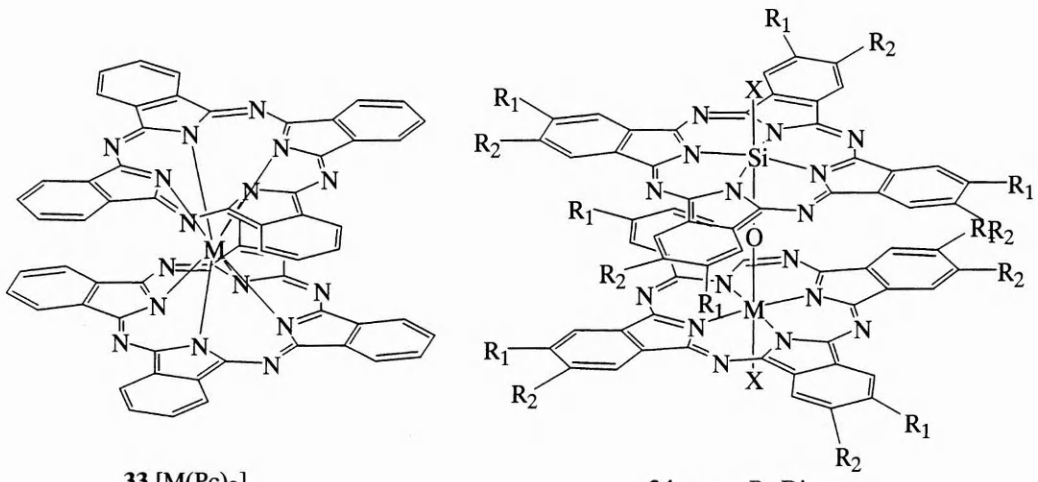

33 $[M(Pc)_2]$ **34** μ-oxo-Pc Dimer

Chart 8

transitions to the upper and lower EX states are forbidden and allowed, respectively. In case of oblique dimers (Figure 13C), there is a dependence on the dihedral angle between the Pc planes. Various studies on ground-state absorption spectra have shown that the transition dipole moments and energy splitting strongly depend on the dimer structure. In case of the cofacial and strongly coupled Pc dimers, an admixture between the EX and CR configurations becomes important. Ishikawa *et al.* have studied the electronic absorption spectra of $[Lu(Pc)_2]^-$ (**33**) and μ-oxo-SiPc dimer (**34**) (Chart 8) by configuration interaction calculations on the localized orbital basis set.[85] For $[Lu(Pc)_2]^-$, the higher energy component band in the Q band region is ascribed to an excitation to an excited state essentially comprising the EX state, while the lower energy component band is assigned as an excitation to that of the CR state, which is granted a spectral intensity from the EX component.

In the T_1 state, the EX interaction is small because of the spin-forbidden transition between the S_0 and T_1 states. The energy transfer occurs via the Dexter mechanism in contrast to the Förster mechanism in the S_1 state. For strongly coupled dimers, the CR contribution is an important factor, even in the T_1 state. The T_1 energy transfer and evaluation of the CR character are discussed in the TREPR section. The admixture between the EX and CR configurations is shown in Figure 14. As a result of the EX interaction, the S_1 states are split into upper and lower EX states, while the T_1 EX splitting is negligibly small. When the ^{1,3}CR energies are higher than the ^{1,3}EX energies, the

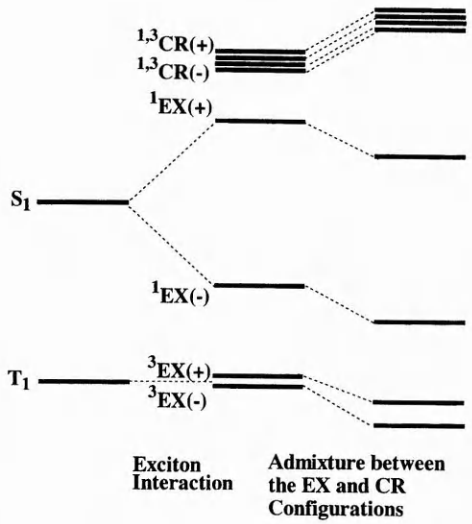

Figure 14. An admixture between the exciton (^{1,3}EX) and charge resonance (^{1,3}CR) configurations.

excited states which mainly consist of ^{1,3}EX configurations shift to the lower energy side, both in the singlet and triplet states.

B. LUMINESCENCE AND TRANSIENT ABSORPTION OF PHTHALOCYANINE DIMERS

Fluorescence emissions have been reported in several Pc dimers. Lever and coworkers have studied the fluorescence emission of several covalently linked H_2Pc dimers (**35–40**, Chart 9).[86] Oddos-Marcel *et al.* have observed fluorescence of μ-oxo-SiPc dimers (**34**, R_1 = methoxy, R_2 = octyloxy, Chart 8).[87] The electronic absorption and fluorescence spectra are shown in Figure 15, and fluorescence peak is seen at around ~940 nm. In contrast to the monomer, the fluorescence of the dimer shifts to lower energy by about 4000 cm^{-1}, while the emission quantum yield is reduced by a factor of 10^{-3}. These energy shift and low fluorescence efficiency of this cofacial dimer are consistent with a forbidden transition between the S_0 and lower EX states, as shown in Figure 13A. The EX splitting is estimated as 3800 cm^{-1} from the electronic absorption and fluorescence spectra.

The transient absorption technique is useful for determining the excited-state dynamics of Pc dimers. The transient absorption data are summarized in Table 9.[20,26,29,30,32,50,88] Rodgers and coworkers have investigated the photophysical properties of cofacial dimers of M-18-CrPc (**41**, Chart 10).[26,50] Cofacial dimerization of H_2-18-CrPc and Zn-18-CrPc by inclusion of Cs^+ ions results in the complete loss of fluorescence, a decrease in the Φ_T values (0.01 and 0.1

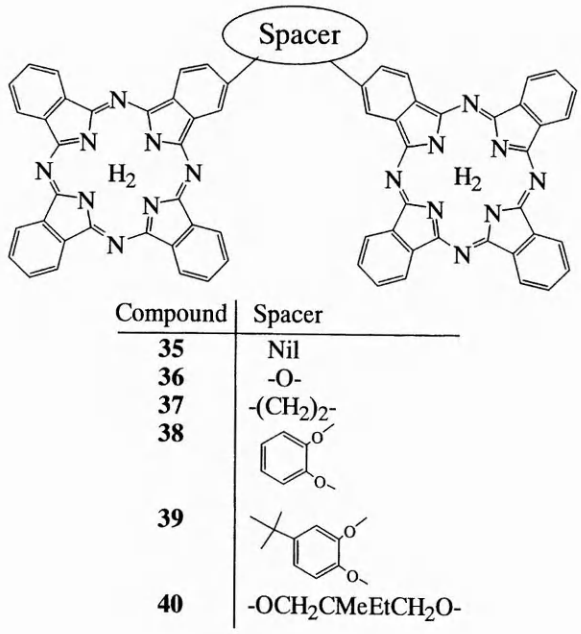

Compound	Spacer
35	Nil
36	-O-
37	$-(CH_2)_2-$
38	
39	
40	$-OCH_2CMeEtCH_2O-$

Chart 9

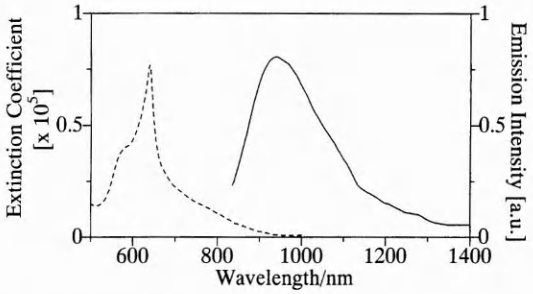

Figure 15. Electronic absorption (broken line) and fluorescence (solid line) spectra of μ-oxo-SiPc dimer in toluene (redrawn from Oddos-Marcel, L.; Madeore, F.; Bock, A.; Neher, D.; Ferencz, A.; Rengel, H.; Wegner, G.; Kryschi, C.; Trommsdorff, H. P. *J. Phys. Chem.* **1996**, *100*, 11850).

for H_2-18-CrPc and Zn-18-CrPc, respectively), and a shortening of the τ_T values. The absence of fluorescence emission in the cofacial dimers is consistent with a rapid decay from the initially-generated upper EX state to the lowest singlet EX state, which is a "dark" state as shown in Figure 13A. The major effect of dimerization is a dramatic increase in IC rates (by a factor of 30–200) and a small enhancement of ISC rates (by a factor of 3–7). This enhancement in IC is attributable to the fact that the lower EX state is close to the ground state, as a result of the EX splitting; in addition, the flexible structures of the cofacial dimers contribute to the IC decay. The increased ISC rate constant is also interpreted by the energy gap law, where the lower EX state approaches the corresponding triplet state in energy.

Table 9. Transient Absorption Data of Phthalocyanine Dimers

Compound number	Central atom/substituents/axial ligand(=X)	Solvent	τ_s/ps	λ_T/nm	$\varepsilon_T/10^3$	Φ_T	τ_T/μs	Ref.
41	H_2/β,(18-crown-6-ether)$_4$	EtOH	113	525	61.3	0.01	120	26
	Co/β,(18-crown-6-ether)$_4$	EtOH	0.8,7.2					50
	Ni /β,(18-crown-6-ether)$_4$	EtOH	2.2,24.2					50
	Cu/β,(18-crown-6-ether)$_4$	EtOH					0.0057	26
	Zn/β,(18-crown-6-ether)$_4$	EtOH	169	525	62	0.10	129	26
34	Si–O–Si/X=(OSi(*n*-hexyl)$_3$)$_2$	$CHCl_3$		500			26	30
	Si–O–Si/R_1=methoxy,R_2=octyloxy/X=OH	Tol		520			90	29
	Si–O–Si/R_1=methoxy,R_2=octyloxy/X=OH	$CHCl_3$		520			100	29
	Si–O–Si/R_1=methoxy,R_2=octyloxy/X=OH	THF		515			130	29
	Si–O–Si/X=(OSi(*n*-hexyl)$_3$)$_2$	Tol	128	500	21.6	0.22	116	20
	Si–O–Ge/X=(OSi(*n*-hexyl)$_3$)$_2$	Tol	197	500	32	0.13	136	20
	Si–O–Sn/X=(OSi(*n*-hexyl)$_3$)$_2$	Tol	103	500	23.3	0.35	32.5	20
33	Lu[a]	CH_2Cl_2	60					88
	Lu[b]	CH_2Cl_2	60					88
	Lu[c]	CH_2Cl_2	36					88
	Sn	ClBz		460			5	32

[a]$[Lu(Pc)_2]^+$. [b]$[Lu(Pc)_2]$. [c]$[Lu(Pc)_2]^-$.

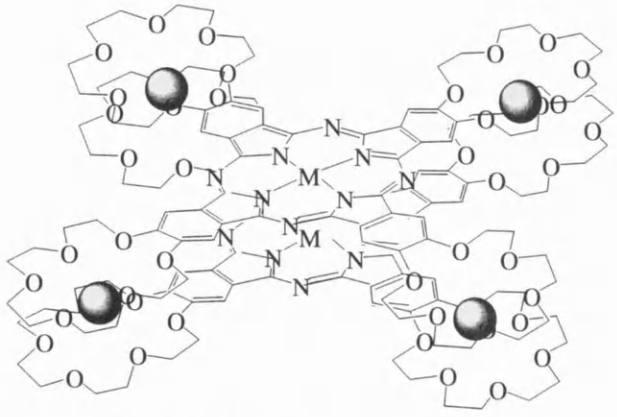

41 M-n-CrPc Dimer
n=18, 18-crown-6 ether substituted Pc
n=15, 15-crown-5 ether substituted Pc

Chart 10

Several groups have reported transient absorption experiments on μ-oxo-MPc dimers (**34**, Chart 8).[20,29,30] Rodgers and coworkers carried out ultrafast pump-probe measurements,[20] in which, prior to 45 ps, changes in transient absorption spectra was detected without isosbestic points. This event is attributed to IC from the upper EX state to the lower EX state, including a vibrational cooling process from the upper tortional/vibrational (hot) state to a thermally equilibrated (cold) state in the lower EX state. The τ_S values were evaluated as 128, 197, and 103 ps for the Si–O–Si, Si–O–Ge, and Si–O–Sn dimers, respectively. The T_1 energy was derived from the energy transfer equilibrium, μ-oxo-dimer $(T_1) + O_2\ (^3\Sigma_g^-) \Longleftrightarrow$ μ-oxo-dimer $(S_0) + O_2\ (^1\Delta_g)$. The T_1 energies were evaluated as ~6600, ~7000 cm^{-1}, and ~7400 cm^{-1} for the Si–O–Si, Si–O–Ge, and Si–O–Sn dimers, respectively, which are much lower than that (~9150 cm^{-1}) of the corresponding monomer. In contrast to the singlet EX interaction, the triplet EX interaction cannot reproduce these lowered T_1 energies, due to the transition dipole moment between the T_1 and S_0 states being negligibly small. The shift in the T_1 energy is reasonably interpreted by the contribution of CR interaction (Figure 14), which has been well demonstrated in several Por dimers.[89,90]

Germain and Ebbesen have investigated $Lu(Pc)_2$ (Chart 8) in three different redox states using transient absorption methods.[88] The excited state lifetimes are very short, being 60, 60, and 36 ps for $[Lu(Pc)_2]^+$, $[Lu(Pc)_2]$, and $[Lu(Pc)_2]^-$, respectively.

C. TIME-RESOLVED ELECTRON PARAMAGNETIC RESONANCE OF PHTHALOCYANINE DIMERS

Recently, TREPR has been shown to be useful for analyzing the EX and CT interactions in T_1 Pc dimers. In this section, we exemplify three kinds of TREPR studies.

We start by discussing the triplet EX state. The EPR of the dimer in the EX state can be classified into three categories, depending on the excitation transfer rate between the constituting Pcs. The first category is a slow-limit case. When the energy transfer rate is much slower than that expected to the zfs energy, the zfs of the dimer is similar to that of the corresponding monomer. The second is a fast-limit case. Sternlicht and McConnel have proposed that the zfs must be averaged over the A and B constituents, when the energy transfer rate is much faster than that expected to the zfs energy.[91]

In this case, the zero field energies are expressed as shown in eq. 8:

$$\begin{pmatrix} X_{EX} \\ Y_{EX} \\ Z_{EX} \end{pmatrix} = \begin{pmatrix} l_x^2 & l_y^2 & l_z^2 \\ m_x^2 & m_y^2 & m_z^2 \\ n_x^2 & n_y^2 & n_z^2 \end{pmatrix} \begin{pmatrix} X_M \\ Y_M \\ Z_M \end{pmatrix} \quad (8)$$

Here, I_{EX} and I_M ($I = X, Y, Z$) denote zero field energies of the triplet sublevels of the dimer in the EX state and the monomer, respectively. l_i, m_i, n_i ($i = x, y, z$) are direction cosines between the fine structure axes (fsa) of the dimer and monomer unit. This equation shows that the zfs in the EX state reflects a structural relationship between the constituting Pc units. In the final category, the energy transfer rate is almost identical to the zfs energy. As shown in Figure 16, resonance magnetic fields of the A and B units (H_A and H_B ($\neq H_A$)) are gradually averaged with increasing energy transfer rate. In this averaging, two EPR signals at around H_A and H_B approach $(H_A + H_B)/2$ with changing linewidth.[92]

Recently, Ishii *et al.* have clearly demonstrated the above three categories using the ZntBPcPy complexes.[93] As shown in Scheme 2, ZntBPcPy forms a self-assembled dimer ((ZntBPcPy)$_2$) in a non-polar solvent, while it reverts to the monomeric form (ZntBPcPy-Py) when Py is added. The TREPR spectra of (ZntBPcPy)$_2$ (20, 100, 140, and 180 K) and ZntBPcPy-Py (20 and 180 K) are shown in Figure 17. The TREPR spectrum of

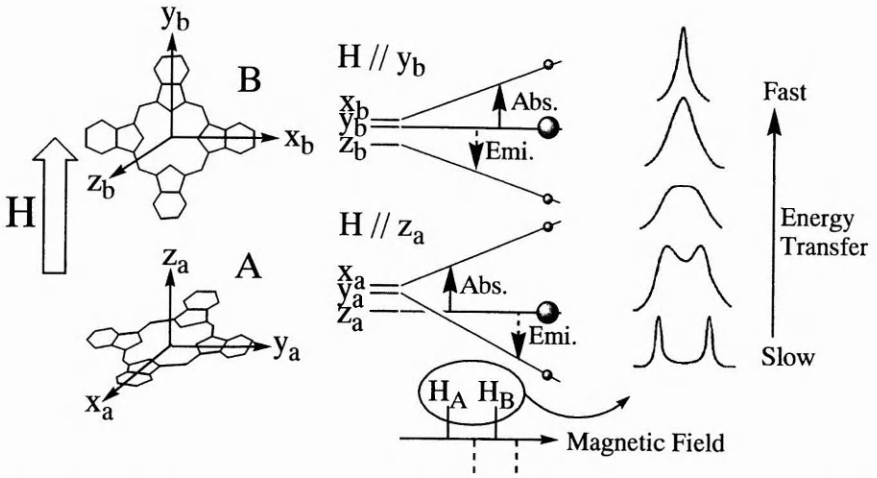

Figure 16. Relationship between the energy transfer rate and EPR signals. Resonance magnetic fields of the A and B units (H_A and H_B; H_A and H_B are EPR transitions when the magnetic field H is parallel to z_a axis of the A unit and y_b axis of the B unit) are gradually averaged with increasing energy transfer rate. In this averaging, two EPR signals at around H_A and H_B approach $(H_A + H_B)/2$ with changing linewidth.

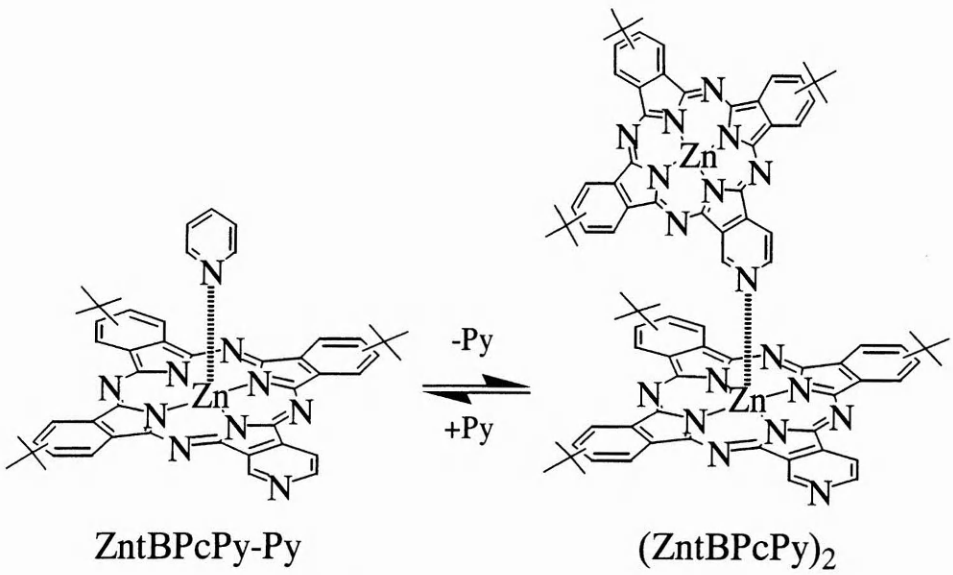

Scheme 2. A self-assembled ZntBPcPy dimer and corresponding monomer.[93]

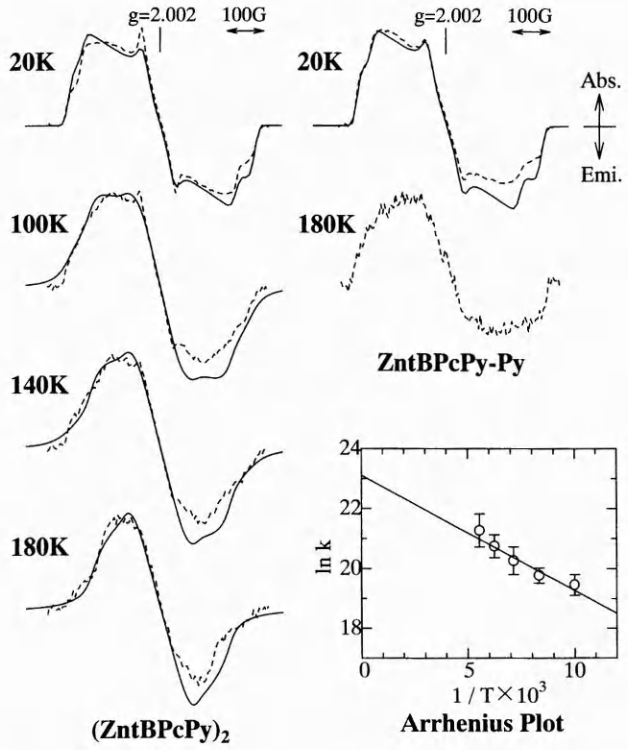

Figure 17. TREPR spectra (dashed lines) of $(ZntBPcPy)_2$ at 20, 100, 140, and 180 K and of ZntBPcPy-Py at 20 and 180 K with their simulations (solid lines). The Arrhenius plot of $\ln k$ vs. $1/T$ is also shown. Simulated spectra of $(ZntBPcPy)_2$ at 100, 140, and 180 K were calculated using $k = 3 \times 10^8$, 7×10^8, and 2×10^9 s^{-1}, respectively.[93]

ZntBPcPy-Py at 20 K was reproduced using the zfs parameters $D = 0.705$ GHz, $E = 0.145$ GHz, and selective ISC to the z sublevel of the T_1 state ($P_x : P_y : P_z = 0 : 0 : 1$), and therefore the T_1 state of ZntBPcPy is assigned to a typical $\pi\pi^*$ configuration. The TREPR spectrum of $(ZntBPcPy)_2$ at 20 K was reproduced using similar parameters ($D = 0.705$ GHz, $E = 0.155$ GHz, and $P_x : P_y : P_z = 0 : 0 : 1$). This similarity shows that the T_1 excitation energy is localized on one constituting unit in the EPR time scale, and that the CT character is negligibly small. On the other hand, a dramatic temperature dependence is seen in the TREPR spectra of $(ZntBPcPy)_2$, where the zfs decreases with increasing temperature. Since the TREPR spectrum of ZntBPcPy-Py at 180 K is very close to that at 20 K, the change in the TREPR spectra of $(ZntBPcPy)_2$ must not be due to the dynamics of the monomer unit, and is, therefore, attributed to energy transfer between the two ZntBPcPy constituents. This is the first and clear EPR demonstration of a pure triplet EX state in porphyrinic derivatives.[94–98] In order to discuss the results quantitatively, spectral simulations, taking the energy transfer process into account, have been carried out. As shown in Figure 17, the TREPR spectra of $(ZntBPcPy)_2$ at 100, 140, and 180 K were well reproduced using the energy transfer rates, $k = 3 \times 10^8$, 7×10^8, and 2×10^9 s^{-1}, respectively. The activation energy of the energy transfer process is evaluated as 2.7×10^2 cm^{-1} from the Arrhenius plot (inset of Figure 17). This analysis exemplifies the utility of the TREPR method for investigating energy transfer processes among these macrocycles.

When both the EX and CR interactions exist in the T_1 state, it is generally difficult to determine the coefficients a and b in eq. 7. Yamauchi and coworkers have studied several cofacial Pc and Por dimers in terms of the admixture between the EX and CR configurations.[37,39,89,99] They have proposed a method for evaluating the CR character using the D value. The D value of the dimer is represented as follows

$$D_{DM} = a^2 D_{EX} + b^2 D_{CR} \tag{9}$$

For parallel cofacial dimers, $l_z = m_z = n_x = n_y = 0$, and $n_z = 1$ in eq. 8, resulting in $D_{EX} = D_M$ ($D = -3Z/2$: Z is the zero field energy of the z sublevel.). Therefore, an important equation is derived as follows.

$$D_{DM} = (1 - b^2) D_M + b^2 D_{CR} \tag{10a}$$

$$b^2 = (D_M - D_{DM})/(D_M - D_{CR}) \tag{10b}$$

From eq. 10b, the contribution of the CR character can be evaluated for the cofacial dimer in the T_1 state. Here, the D_M and D_{DM} values are evaluated from the TREPR measurements, and the D_{CR} value is calculated under a point charge approximation. The TREPR parameters are summarized in Table 10.[35,37,39,93] In the case of M-15-CrPc (**41**, Chart 10) (M = H_2, Zn), the D values decrease with dimerization. Furthermore, the D values of the $[M(Pc)_2]^-$ species (Chart 8) are much smaller than those of the corresponding monomers. These decreases in the D value can be attributed to the contribution of the CR character, since the D value of the parallel dimer is unchanged by the EX interaction. Using eq. 10b, the contribution of the CR character, b^2, is evaluated as 0.070, 0.093, 0.27, and 0.47, for $(H_2\text{-}15\text{-}CrPc)_2$, $(Zn\text{-}15\text{-}CrPc)_2$, $[Y(Pc)_2]^-$, and $[Lu(Pc)_2]^-$, respectively, which correlates well with the interplanar distance. This is consistent with theory, where the admixture between the EX and CR configurations depends on the coulombic and resonance integrals between two Pc units.[99,100]

Ishii *et al.* have investigated planar and conjugated Pc dimers, in which two Pcs (**42**, PcPc) or one Pc and pyrazinoporphyrazine (**43**, PcPyz) strongly interact with each other through a common benzene ring (Chart 11).[35] TREPR spectra of H_2tBPc, PcPc, and PcPyz are shown in Figure 18. As summarized in Table 10, the D value of PcPc is much smaller than that of H_2tBPc. This decrease

Table 10. Zfs Parameters and Sublevel Population Ratios of Phthalocyanine Dimers

Compound name or number	Central atom/substituents	D^a/GHz	E^b/GHz	$P_y : P_x : P_z$	Ref.
$(ZntBPcPy)_2$		0.705	0.155	0:0:1	93
41	H_2/β,(15-crown-5-ether)$_4$	0.71	0.06	0.5:0.5:0	37
	Zn/β,(15-crown-5-ether)$_4$	0.69	0.08	0:0.2:0.8	37
33	Y	0.40	0.13	0:0:1	39
	Lu	0.21	0.11	0:0:1	39
42		0.645	0.105	0.35:0.65:0	35
43		0.480	0.040	0.4:0.6:0	35

[a] $D=-3Z/2$. [b] $E=|X-Y|/2$. X, Y, and Z are zero field energies of the x, y, and z sublevels, respectively.

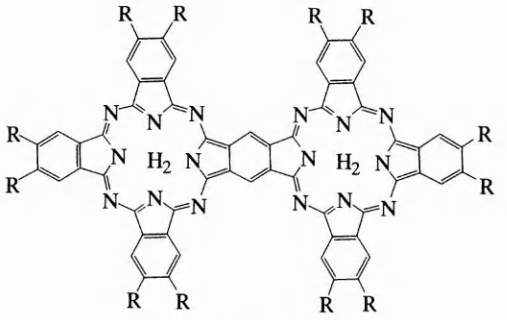

42 PcPc
R = $OCH_2CHEt(CH_2)_3CH_3$

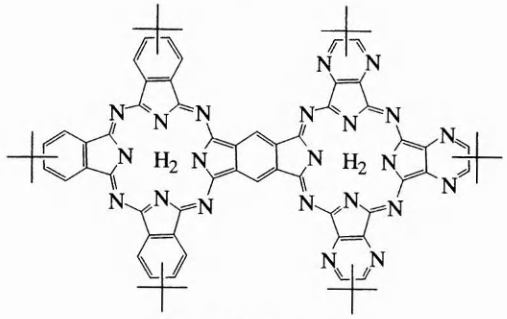

43 PcPyz

Chart 11

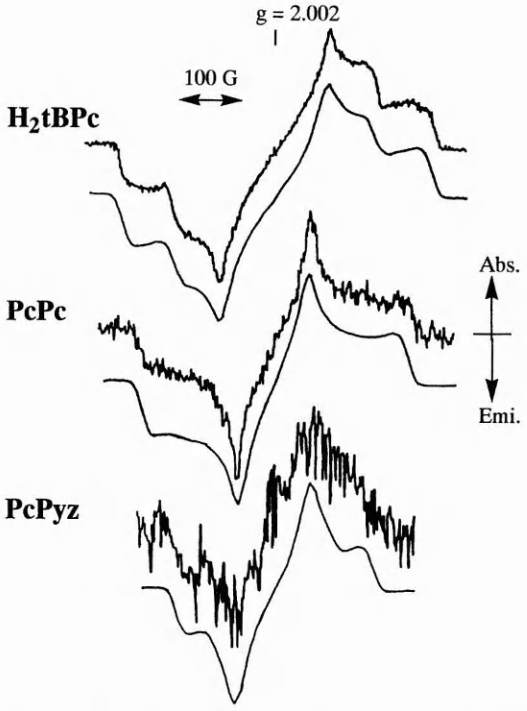

Figure 18. TREPR spectra of H_2tBPc, PcPc, and PcPyz with their simulations (lower). These spectra were observed at 20 K and 0.5 μs after laser excitation.[35]

can be explained by a delocalization of excitation over two Pc units in the T_1 state. This is supported by MO calculation of PcPc, where the π electrons of the HOMO and LUMO delocalize over the two Pc units. In order to discuss the effects quantitatively, D values were calculated under a half-point charge approximation. The calculated D value (0.426 GHz) of PcPc is smaller than that (0.605 GHz) of Pc, in analogy with the experimental results. Furthermore, the D value (0.480 GHz) of PcPyz is smaller than that of PcPc, and cannot be interpreted simply by the expansion of π delocalization in the T_1 state. The MO calculations of the monomers suggest that the HOMO (−7.49 eV) and LUMO (−3.74 eV) of Pc are higher than the HOMO (−7.98 eV) and LUMO (−4.02 eV) of Pyz, respectively. In fact, the electron density on the Pc ring is larger than that on the Pyz ring for the HOMO of PcPyz, while it is smaller for the LUMO. Therefore, the small D of PcPyz originates from the contribution of a CT configuration between Pc and Pyz. The calculated D value of PcPyz is smaller than that of PcPc, in accordance with the experimental trend.

D. PHTHALOCYANINE OLIGOMERS

The photophysics of several cofacial Pc oligomers (**44**–**46**, Chart 12) has been investigated in solution, and in their columnar liquid-crystalline (LC) and crystalline phases, in terms of exciton hopping and exciton–exciton annihilation. Ern *et al.* have studied the femtosecond transient absorption of Pcpolysiloxane (**44**, Chart 12).[101] This linear polymer consists of an average of 32 cofacially stacked μ-oxo-bridged SiPc rings with

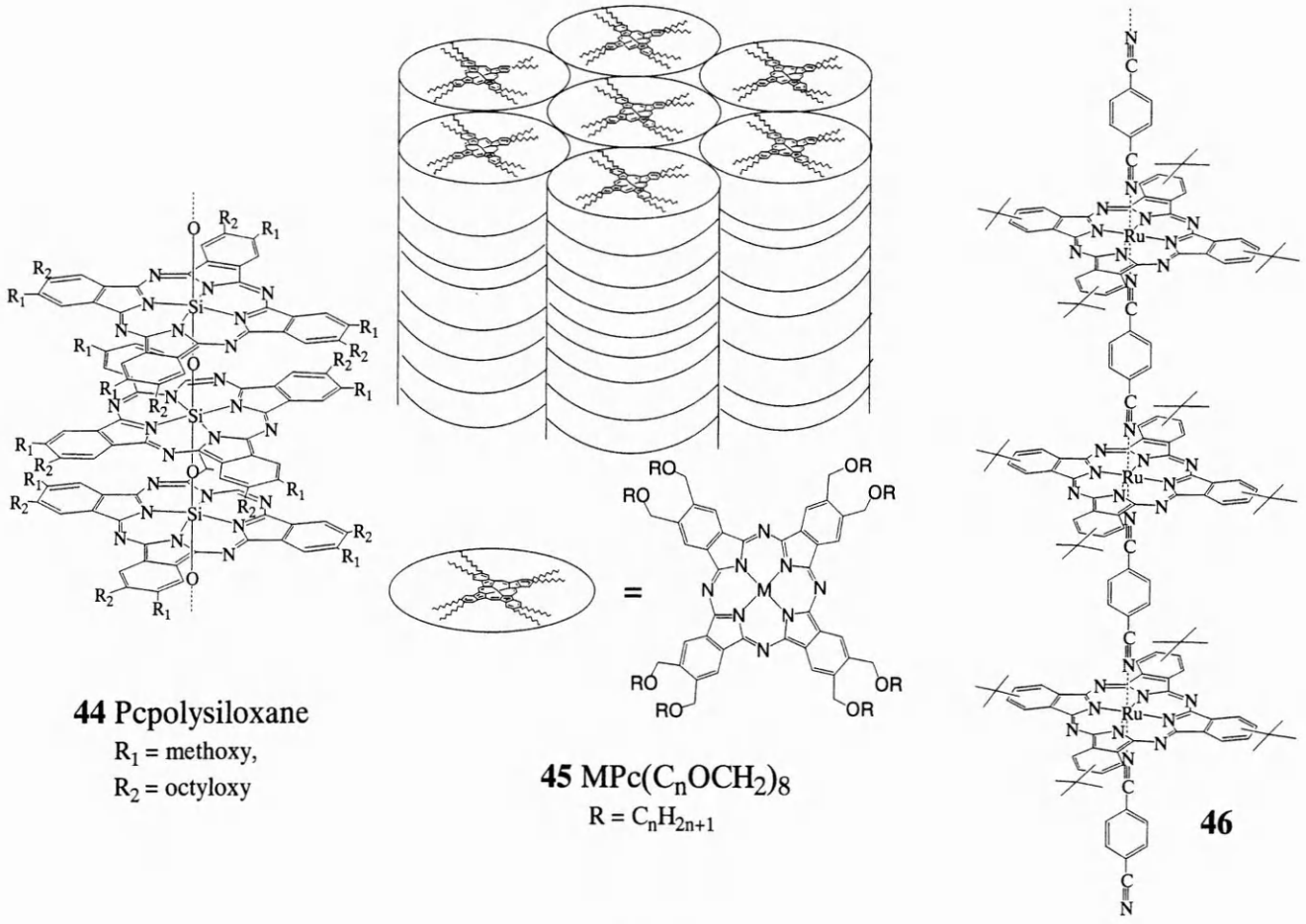

Chart 12

stacking distances of $d_{Si-O-Si} = 0.33$ nm, constituting fairly rigid rods of *ca.* 11 nm length. Both photoinduced bleaching and transient absorption are observed, and the decay dynamics, which strongly depend on the excitation energy density, are non-exponential. It is found that the excited state lifetime of singly excited chains is *ca.* 4.5 ps, dropping to about 0.5 ps for doubly excited chains and becoming less than the instrumental resolution of 150 fs at higher excitation densities. This indicates that at higher excitation densities, the observed relaxation dynamics in SiPc are dominated by exciton–exciton annihilation.

Photophysical properties of the octakis(alkoxymethyl) metal-free and zinc Pcs (**45**, Chart 12) have been studied in their crystalline and columnar LC phases. Simon and coworkers have studied the fluorescence properties of $H_2Pc(C_{12}OCH_2)_8$.[102] From the fluorescence quenching in the presence of copper complexes, the exciton diffusion length is estimated as 100–200 Å in the crystal. In the LC, the fluorescence efficiency is very low in the absence of the copper complex, and is related to a more disorganized state. Markovitsi *et al.* have carried out nanosecond and picosecond time-resolved absorption measurements.[103–105] For low laser pulse energies (< 0.6 mJ) the transient optical density is a linear function of the exciting pulse energy: at higher energies saturation is observed. The transient optical density in the crystal is 3.7 times greater than that in the LC. It can be assumed that this is mainly due to a difference in the Φ_T rather than a difference in the ε_T, since the ε_{max} observed for the singlet–singlet transition does not change with the phase transition. The transient decay kinetics observed with low-energy excitation is single-exponential, with τ_T values evaluated as 21.5 and 10.0 μs for the crystal and LC, respectively. At high excitation energy, the transient decay fits second-order kinetics, i.e. T–T annihilation. The second order rate remains almost constant over the crystalline-phase temperature domain, 1.0×10^6 s^{-1}, but it increases dramatically to 13.0×10^6 s^{-1} when the LC phase is formed. This difference shows that T–T annihilation is more rapid in the LC state than in the crystal. In the initial stages, the triplet state population varies as $t^{-1/2}$, which is characteristic of diffusion-limited

one-dimensional T–T annihilation. The long time decays are well described by a random walk model on a linear chain containing traps. It is possible to determine an order of magnitude for the EX hopping time (τ_{EX}) by two independent methods, based either on the short-time or the long-time decay kinetics. In the case of a short-time decay, τ_{EX} is obtained using the slope of the $1/\Delta OD$ vs. $t^{1/2}$ plots. The τ_{EX} values in the crystal are evaluated as 40, 45, and 46 ps for $H_2Pc(C_{12}OCH_2)_8$, $ZnPc(C_{12}OCH_2)_8$, and $H_2Pc(C_{18}OCH_2)_8$, respectively. The τ_{EX} values in the LC are 7.4, 0.4, and 66 ps for $H_2Pc(C_{12}OCH_2)_8$, $ZnPc(C_{12}OCH_2)_8$, and $H_2Pc(C_{18}OCH_2)_8$, respectively. On the other hand, from the long-time decays, the τ_{EX} values in the crystal are evaluated as 28, 42, and 34 ps for $H_2Pc(C_{12}OCH_2)_8$, $ZnPc(C_{12}OCH_2)_8$, and $H_2Pc(C_{18}OCH_2)_8$, respectively. The τ_{EX} values in the LC are 9.5, 0.4, and 68 ps for $H_2Pc(C_{12}OCH_2)_8$, $ZnPc(C_{12}OCH_2)_8$, and $H_2Pc(C_{18}OCH_2)_8$, respectively. The τ_{EX} values determined from the short decay kinetics are in agreement with those determined independently from the long-time behavior of the triplet decay. The hopping time is found to be faster in the LC than in the crystal by at least a factor 5 for $H_2Pc(C_{12}OCH_2)_8$ and a factor of 110 for $ZnPc(C_{12}OCH_2)_8$, except for $H_2Pc(C_{18}OCH_2)_8$ which exhibits a structural similarity between the mesophase and metastable crystalline phase. Moreover, the exciton diffusion coefficient is higher in the LC than in the crystal, consistent with a more efficient energy migration in the LC than in the crystal.

Markovitsi *et al.* have also studied the photophysical properties of a soluble oligomeric RutBPc (**46**, Chart 12) in which the macrocycles are axially linked to a bidentate bridging ligand, *p*-diisocyanobenzene, in comparison with that of monomeric analogue.[106] Two different oligomers corresponding to an average degree of polymerization of 25 and 46, have been investigated, in which the centre-to-centre distance between two neighboring Pc units in the oligomeric chains is *ca.* 12 Å. The triplet-decay kinetics are single exponential, yielding lifetimes of 6.3 μs for RutBPc(*t*-butylisonitrile)$_2$ and 8.5 μs for [RutBPc(*p*-diisocyanobenzene)]$_n$. In the oligomer case, the triplet decay becomes single-exponential only when the triplet molar ratio, C_T/C_0 (C_T and C_0 are the triplet and ground-state concentrations, respectively), is reduced to 0.20. As the average degree of polymerization is 25 (or 46), each triplet state decays independently when each polymeric chain contains less than five (or nine) triplet states. Under these conditions, the absence of a bimolecular deactivation process proves that triplet migration is inefficient in the polymeric chains; i.e., the triplet-hopping time must be long compared to the triplet lifetime. At high excitation intensities, direct T–T annihilation, which is not diffusion limit, is observed. It is shown that T–T interactions are probably effective at distance of at least 24 Å.

Using fluorescence and electronic absorption, Kobayashi *et al.* have investigated the aggregation of amphiphilic ZnPc substituted by eight tri(ethylene oxide) chains (ZnEGPc) in water, dioxane, and dioxane/water mixtures.[107] The electronic absorption spectra broaden with increasing proportion of water, indicating aggregation of ZnEGPc. On the other hand, the change in the shape of the S_1 emission spectrum is relatively small, while the Φ_F value decreases with increasing ratio of water. Since the τ_F and oscillator strength of the Q_{0-0} band are independent of hydration, the decrease in the Φ_F value is attributed to the aggregation of ZnEGPc. That is, the Φ_F value reflects the population ratio of aggregates. It is clearly demonstrated that the degree of aggregation depends on the proportion of water.

E. PHTHALOCYANINE-PORPHYRIN HETEROOLIGOMERS

The photophysical behaviors of various Pc–Por heterooligomers has been studied in relation to electron or energy transfer processes. Tran-Thi *et al.* have investigated several Pc–Por heterodimers, using fluorescence and transient absorption measurements.[108–111] Intramolecular transfer processes in a covalently linked ZnPc–ZnTTP (**47**, Chart 13) have been investigated as a function of the solvent polarity.[108] In toluol, selective excitation of the porphyrin chromophore is followed by a very efficient energy-transfer process to the Pc moiety. The energy transfer efficiencies are 0.87 and 0.88 in the excited singlet and triplet states, respectively. In contrast to this phenomenon, a CT reaction occurs in DMSO. The quantum yields of the electron transfer is 0.84 from both the S_1 ZnTTP and S_1 ZnPc. This difference in solvent originates from the stabilization of the CT energy in polar DMSO, resulting in an efficient electron transfer from the S_1 state. In contrast to the excited singlet behavior, energy transfer from ZnTTP to ZnPc occurs in the T_1 state. This inefficient CT from the T_1 state is consistent with the fact that the T_1 energy is much lower than the S_1 energy. The excited state dynamics of ZnPc–ZnTTP has clearly illustrated the dependence on solvent polarity. A subpicosecond time-resolved absorption measurement has been carried out for Ce(Pc)(TPP) (**48**, Chart 13).[109]